J. Fluid Mech. (1997), *vol.* 342, *pp.* 377–401. Printed in the United Kingdom

Breaking waves and the equilibrium range of wind-wave spectra

By S. E. BELCHER[1] AND J. C. VASSILICOS[2]

[1]Department of Meteorology, University of Reading, Reading RG6 6AH, UK

[2]Department of Applied Mathematics and Theoretical Physics, University of Cambridge, Silver Street, Cambridge CB3 9EW, UK

(Received 11 October 1996 and in revised form 27 February 1997)

When scaled properly, the high-wavenumber and high-frequency parts of wind-wave spectra collapse onto universal curves. This collapse has been attributed to a dynamical balance and so these parts of the spectra have been called the equilibrium range. We develop a model for this equilibrium range based on kinematical and dynamical properties of breaking waves. Data suggest that breaking waves have high curvature at their crests, and they are modelled here as waves with discontinuous slope at their crests. Spectra are then dominated by these singularities in slope. The equilibrium range is assumed to be scale invariant, meaning that there is no privileged lengthscale. This assumption implies that: (i) the sharp-crested breaking waves have self-similar shapes, so that large breaking waves are magnified copies of the smaller breaking waves; and (ii) statistical properties of breaking waves, such as the average total length of breaking-wave fronts of a given scale, vary with the scale of the breaking waves as a power law, parameterized here with exponent D.

The two-dimensional wavenumber spectrum of a scale-invariant distribution of such self-similar breaking waves is calculated and found to vary as $\Psi(\boldsymbol{k}) \sim k^{-5+D}$. The exponent D is calculated by assuming a scale-invariant dynamical balance in the equilibrium range. This balance is satisfied only when $D = 1$, so that $\Psi(\boldsymbol{k}) \sim k^{-4}$, in agreement with recent data. The frequency spectrum is also calculated and shown to vary as $\Phi(\sigma) \sim \sigma^{-4}$, which is also in good agreement with data. The theory also gives statistics for the coverage of the sea surface with breaking waves, and, when $D = 1$, the fraction of sea surface covered by breaking waves is the same for all scales. Hence the equilibrium described by our model is a *space-filling saturation*: equilibrium at a given wavenumber is established when breaking waves of the corresponding scale cover a given, wind-dependent, fraction of the sea surface.

Although both $\Psi(\boldsymbol{k})$ and $\Phi(\sigma)$ vary with the same power law, the two power laws arise from quite different physical causes. As the wavenumber, k, increases, $\Psi(\boldsymbol{k})$ receives contributions from smaller and smaller breaking waves. In contrast, $\Phi(\sigma)$ is dominated by the largest breaking waves through the whole of the equilibrium range and contains no information about the small-scale waves. This deduction from the model suggests a way of using data to distinguish the present theory from previous work.

1. Introduction

Since the pioneering work of Phillips (1958) there has been considerable interest in the high-wavenumber and the high-frequency tails of the wavenumber and the

frequency spectra of ocean waves. These parts of the spectra, with wavenumber or frequency greater than about three times the values at the peaks in the spectra, are of inherent scientific interest because data show that, when scaled properly, they collapse onto universal curves (e.g. Phillips 1977, p. 140). Phillips (1958) called this a saturation range, whereas Kitaigorodskii (1983) and Phillips (1985) used the term equilibrium range. The smaller-scale waves that control these parts of the spectra are important because they largely determine the momentum exchange between the atmosphere and the ocean (e.g. Makin, Kudryatsev & Mastenbroek 1995). And recently this equilibrium range has increased in practical significance following developments in remote sensing.

Previous studies have suggested different forms for the equilibrium range of the wavenumber spectrum, $\Psi(\boldsymbol{k})$, and the frequency spectrum, $\Phi(\sigma)$. All of these forms have a power-law variation with wavenumber k or frequency σ. For example, for the wavenumber spectrum Phillips (1958) suggested $\Psi(\boldsymbol{k}) \sim \text{const} \times k^{-4}$, and Kitaigorodskii (1983) and Phillips (1985) have proposed $\Psi(\boldsymbol{k}) \sim \text{const} \times u_* \mathrm{g}^{-1/2} k^{-7/2}$ (where u_* is the friction velocity and g is the gravitational acceleration). Meanwhile, a recent survey of data by Banner (1990) revealed that $\Psi(k, \theta_0) \sim \text{const} \times (U_0/c_p)^{1/2} k^{-4}$, where θ_0 is the wind direction, U_0 is a reference surface wind speed and c_p is the phase speed of waves at the peak in the spectrum. Similarly, power-law forms have been proposed for the high-frequency part of the frequency spectrum. Phillips (1958) suggested $\Phi(\sigma) \sim \text{const} \times \mathrm{g}^2 \sigma^{-5}$. And the models of Kitaigorodskii (1983) and Phillips (1985) give $\Phi(\sigma) \sim \text{const} \times u_* \mathrm{g} \sigma^{-4}$, which agrees well with measurements made by Toba (1973) and other data presented in Phillips (1985). So, although the theoretical models of Kitaigorodskii (1983) and Phillips (1985) seem to agree with the data for $\Phi(\sigma)$, their models for $\Phi(\sigma)$ were derived from the theoretical results for $\Psi(\boldsymbol{k})$ that do not agree with current data. In contrast, Phillips' (1958) model gives a k^{-4} variation, which agrees with the current data, but his inferred frequency spectrum does not. Hence no current theory can give the variation of both the wavenumber and frequency spectra in the equilibrium range that agree with current best estimates from data. The aim of the present paper is to develop a theory for the equilibrium range of wind waves that is consistent with $\Psi(\boldsymbol{k}) \sim k^{-4}$ and $\Phi(\sigma) \sim \sigma^{-4}$.

To examine this question consider first how the sea surface could be reconstructed from the wavenumber spectrum. One approach is to model the sea surface as a collection of sinusoidal waves with amplitudes chosen to give the correct spectrum and to assume that the phases of the sinusoidal waves are random so that the surface has a Gaussian probability distribution (Pierson 1955). When the spectrum has a power-law variation, such a surface has a fractal geometry (a result originally found by Orey 1970, and more recently discussed in the context of ocean waves by Glazman & Weichman 1989).

Although the random-phase model does capture some aspects of the sea surface, important elements are missing. Firstly, measurements of the probability density function of the surface elevation show a marked non-Gaussian behaviour; see, for example, the measurements made by Kinsman, which are shown in Phillips (1977, p. 185). The deviations from a Gaussian distribution are qualitatively consistent with the wave crests being sharper than the wave troughs. Secondly, quantitative analysis of time series of surface-elevation data using wavelet transforms show crests that are sharper than the troughs and indicate that occasionally there are wave crests with large curvature, and hence nearly discontinuous slopes (Shen, Wang & Mei 1994). Such waves are probably on the point of breaking (at least according to the development shown by the photographs in Rapp & Melville 1990).

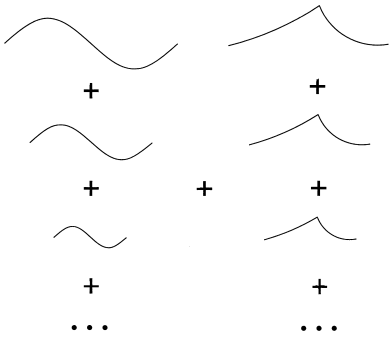

FIGURE 1. The wave field as a superposition of sinusoids plus sharp-crested breaking waves.

Following Shen *et al.* (1994), the picture that we propose is of the surface waves being composed of smooth-crested waves, together with breaking waves with sharp crests (figure 1). In contrast, most previous models of the equilibrium range (e.g. Phillips 1958, 1985; Kitaigorodskii 1983) have assumed that the sea surface is a collection of sinusoidal water waves that propagate according to the linear dispersion relation. Wave breaking certainly becomes more frequent at small scales as shown, albeit indirectly, by the high values of dissipation of wave energy at high frequencies in wave forecast models (see e.g. Komen, Hasselmann & Hasselmann 1984). Here we assume that the geometry and dynamics of breaking waves play the controlling role in the equilibrium range and we develop a model for the equilibrium range based on geometrical and dynamical properties of such breaking waves.

1.1. *Properties of breaking waves*

Sharp-crested breaking waves play a central role in the calculations developed in this paper and so experimental measurements of breaking waves are now reviewed and interpreted to motivate the idealized model used in our calculations. A review of the recent developments in breaking waves is given by Banner & Peregrine (1993), and a review of the role of breaking waves in the air–sea interaction has been written by Melville (1996).

Laboratory experiments have been used to examine geometrical properties of breaking waves. Bonmarin (1989) used a mechanical wavemaker to generate waves with wavelengths on the order of a metre and examined how some geometrical properties of the waves varied as the waves broke. These experiments show that immediately preceeding and during breaking there is a region of high curvature at the wave crest. Shen *et al.* (1994) generated wind waves in a laboratory flume, producing dominant waves with wavelengths of the order of 0.5 m, they also obtained field data with dominant wavelengths of the order of 5 m. They then performed wavelet analyses on time series of the surface elevation measured at a point in these wave fields. Their analysed data show wave crests with very high curvature, which suggests that such sharp crests occur in wind-generated waves and are not an artifact of Bonmarin's mechanical method of generating breaking waves. These experiments suggest an idealized model that is used here to represent the breaking waves. The curvature at the breaking-wave crest is taken to be infinite, so that the slope of the water surface is discontinuous at the crest. Such waves are denoted here as Λ-crests. In two dimensions the wave field therefore has lines of breaking-wave fronts along which the slope is discontinuous.

Further information on the properties of breaking waves is provided by the interesting experiments performed by Duncan (1981), who generated continuously overturning breaking waves with wavelengths of the order of 0.5 m by towing a submerged hydrofoil through water. These experiments show that the geometry of quasi-steady breaking waves is statistically self-similar, so that on average the larger breakers are magnified copies of the smaller breakers. In addition Duncan's (1981) experiments show that, amazingly, the breaking region itself is a fixed fraction of the cross-sectional area of the wave, and so is also statistically self-similar. Although we know of no direct evidence that the transient breakers in wind-generated waves are also self-similar, Duncan's (1981) experiments are at least suggestive. Hence we use self-similar Λ-crests to model the transient breaking waves on the ocean.

Duncan (1981) used his measurements to determine a scaling for the rate that wave energy is dissipated by a continuously breaking wave. Melville (1994) re-examined data on unsteady breakers and suggested that this scaling remains valid for transient breakers produced in the laboratory, although he does urge caution since some of the measurements are prone to substantial error. Nevertheless, that there is some agreement between the two scalings suggests that experiments with continuously breaking waves give at least some illustration of the properties of transient breakers. In §3 we use the form of the scaling derived by Duncan (1981) to estimate dissipation of wave energy by transient breaking waves.

Ding & Farmer (1994) tracked breaking waves in a field experiment using an array of hydrophones. These experiments confirm that breaking in an active wind sea occurs on a wide range of scales. Hence our model of the equilibrium range is a summation of self-similar Λ-crests with a whole distribution of lengthscales.

The model developed here is based on the assumption that the equilibrium range of the wind waves is scale-invariant. This assumption is used extensively in this paper and has three major implications: it implies that Λ-crests must be statistically self-similar; it establishes how the distribution of Λ-crests can vary with scale; and it has implications for the dynamical balance that is possible in the equilibrium range. These aspects are addressed next.

1.2. *Scale invariance, self-similarity and spectra*

Spectra have traditionally been used to identify characteristic frequencies or wavenumbers where significant wave activity is concentrated. But when a spectrum takes a power-law form, e.g. $\Psi(\boldsymbol{k}) \sim k^{-p}$, then there exists no privileged or characteristic Fourier mode in the range of wavenumbers where this power law holds. To understand this statement consider the ratio of the energy in wavenumbers between k and $k + \mathrm{d}k$ to the energy between the scaled wavenumbers sk and $s(k + \mathrm{d}k)$. This ratio is $k^{-p}\mathrm{d}k/(sk)^{-p}\mathrm{d}(sk) = s^{p-1}$, which does not depend on the reference wavenumber k but only on the scaling factor s: hence no wavenumber is special. The absence of characteristic wavenumbers or frequencies in power-law spectra suggests that characteristic length- or timescales are also absent from the geometry and dynamics of the underlying wave field. Such geometry and dynamics are called here *scale invariant*†. Experimentally measured wavenumber and frequency spectra show equilibrium ranges with power-law forms, which suggests that the geometry of the sea surface and the dynamical balance in the equilibrium range might both be scale invariant.

† Scale invariance and self-similarity are often used synonymously in the literature. Here 'self-similar' is used to mean that waves of different sizes are, statistically, geometrically similar in shape; whereas 'scale invariance' is used to denote the more general notion of absence of privileged length- or timescales.

Hence the most decisive assumption made in this paper is that, in the equilibrium range of wind waves, both the geometry and the dynamical balance are scale-invariant. This assumption has two implications for the geometry of the surface waves. The first implication is that sharp-crested breaking waves are, on average, geometrically self-similar (otherwise a special lengthscale would be introduced). But the sea surface is composed of breaking waves of a whole range of scales, and the second implication concerns $M(l)\mathrm{d}l$, which is defined to be the number of breaking waves with sizes between l and $l + \mathrm{d}l$ *per unit area* of sea surface. One simple reason to motivate why $M(l)$ might vary with l is that the number of breaking waves that can be fitted into a unit area without overlapping is proportional to l^{-2}, which yields $M(l)\mathrm{d}l \propto l^{-2}$. The actual variation is likely to be different and physically $M(l)$ is determined by the dynamics of the wave field, i.e. the dynamical interplay between wind and waves, wave–wave interactions and dissipation due to wave breaking. However the assumption of scale invariance is enough to determine the functional form of $M(l)$.

In general, dimensional considerations require that $M(l)$ depends on l and a reference lengthscale l_0, so that $M(l)\mathrm{d}l = l_0^{-2}\hat{M}(l/l_0)\mathrm{d}(l/l_0)$, where $\hat{M}(l/l_0)$ is a dimensionless function of l/l_0. The assumption of scale invariance of the sea-surface geometry means that the ratio $\hat{M}(l_1/l_0)/\hat{M}(l_2/l_0)$ for two different crest sizes l_1 and l_2 is independent of l_0, i.e. l_0 is not a characteristic lengthscale (cf. the argument given above that if the spectrum varies as a power law then it is scale invariant). This condition of scale invariance can be written

$$\frac{\mathrm{d}}{\mathrm{d}l_0}\left\{\frac{\hat{M}(l_1/l_0)}{\hat{M}(l_2/l_0)}\right\} = 0. \tag{1.1}$$

The only solution to this equation is that $\hat{M}(l)$ varies as a power-law dependence on the crest size l, which we write for later convenience as

$$\hat{M}(l) = (l_0/l)^{D+2}. \tag{1.2}$$

The lengthscale l_0 is defined to be the 'outer' lengthscale of the equilibrium range, i.e. the lengthscale of the largest breaking waves. Equation (1.2) introduces the scaling exponent D that we use to parameterize the scale-invariance of the sea surface. A sum of self-similar Λ-crests with a distribution like (1.2) will then be scale invariant and so will lead to spectra that vary as power laws.

1.3. *Development of the model*

The geometry of a spatial configuration must be quite particular for that geometry to be statistically scale invariant. Yet the correct description and parameterization of scale-invariant geometries is not generally known. Nor is the relation of power-law spectra to these scale-invariant geometries generally well understood, although there are a few special cases where they are, e.g. fractal Brownian motions (Orey 1970), statistically homogeneous and isotropic sharp interfaces (Vassilicos & Hunt 1991), spiral interfaces (Gilbert 1988; Vassilicos 1995). Here we perform calculations that add to this list and the scale-invariant geometry of the sea surface is parameterized by the exponent D and a relationship is established between D and the wavenumber spectrum.

In §2 a kinematic analysis is used to calculate the two-dimensional wavenumber spectrum of a scale-invariant distribution of self-similar sharp-crested breaking waves. The model is constructed in a number of stages. First, a one-dimensional slice through the two-dimensional wave surface is considered, and in §2.2 we explain how the

discontinuity in the slope at the sharp crests leads to a one-dimensional spectrum that decays as k^{-4}. In §2.3 we explain how a scale-invariant variation in the distribution of a set of sharp-crested waves with their discrete scales changes the power-law decay of the one-dimensional wavenumber spectrum. These arguments are generalized in §2.4 to account for sharp-crested waves with a continuous range of scales. Finally in §2.5 these calculations are further generalized to compute the two-dimensional wavenumber spectrum of the two-dimensional sea surface that carries a continuous distribution of breaking-wave fronts. The key result is that the two-dimensional wavenumber spectrum varies as k^{-5+D}. Purely kinematical ideas cannot fix D, so in §3 we develop dynamical ideas based on the assumption that the dynamical processes are scale invariant and on the notion that the high-wavenumber part of the spectrum is in a local balance and thence fix the value of D. Physical interpretation of these results and the wavenumber spectrum is given in §4. Then in §5 the frequency spectrum is calculated using the one-dimensional kinematical theory together with the value of D determined in §3. Finally we draw conclusions in §6.

2. Kinematics of sharp-crested breaking waves

Consider first a one-dimensional slice through the two-dimensional wave field, and suppose that the elevation of the water surface at a given fixed time and at position x along the slice is $\zeta(x)$. As discussed in §1, the surface elevation is modelled here as a combination of smooth waves, denoted by $\zeta_s(x)$, together with sharp-crested breaking waves (figure 1). Denote a breaking wave of horizontal scale l_n (such that $l_n < l_m$ if $n > m$), and centred at x_{nm}, by $\Lambda_{nm}(x - x_{nm}, l_n)$. In principle the individual sharp crests could have different shapes, hence the subscripts on Λ_{nm}. On dimensional grounds, if l_n is the only horizontal scale of the wave, then the Λ-crest is a function of $(x - x_{nm})/l_n$. The surface elevation can then be written

$$\zeta(x) = \zeta_s(x) + \sum_{n,m} a_{nm}\Lambda_{nm}((x - x_{nm})/l_n), \tag{2.1}$$

where a_{nm} is the amplitude of the crest of size l_n at x_{nm}.

Using the convolution theorem, the one-dimensional wavenumber spectrum, $\Psi_1(k)$, can be related to the Fourier transform of the wave elevation along the slice:

$$\Psi_1(k) \equiv \int \overline{\zeta(x_0)\zeta(x_0 + x)}\, \mathrm{e}^{\mathrm{i}kx}\, \mathrm{d}x = \frac{(2\pi)^2}{L_x}\overline{|\tilde{\zeta}(k)|^2}, \tag{2.2}$$

where overbar denotes averaging over realizations and over the reference position x_0 from 0 to L_x (L_x is the length of the record); $\tilde{\zeta}(k)$ is the Fourier transform of $\zeta(x)$, defined by

$$\tilde{\zeta}(k) = \frac{1}{2\pi}\int \zeta(x)\, \mathrm{e}^{\mathrm{i}kx}\, \mathrm{d}x. \tag{2.3}$$

Hence calculation of $\Psi_1(k)$ reduces to calculating the Fourier transform of the wave elevation.

2.1. *Fourier transform of a Λ-crest*

The Fourier transform of a Λ-crest is now calculated. The main features of this Fourier transform arise from the discontinuity in slope at the crest and the overall scale l_n; it is not necessary to define the shape of a Λ-crest more precisely.

Following Lighthill (1958, theorem 19), the behaviour of the Fourier transform of

Λ_{nm}, denoted by $\tilde{\Lambda}_{nm}$, at large k can be established by integrating by parts:

$$\tilde{\Lambda}_{nm}(k, l_n, x_{nm}) = \frac{1}{2\pi}\int \Lambda_{nm}((x - x_{nm})/l_n)\,\mathrm{e}^{\mathrm{i}kx}\,\mathrm{d}x$$
$$= \frac{1}{2\pi} l_n \mathrm{e}^{\mathrm{i}\phi_{nm}} \frac{1}{(kl_n)^2}\{\alpha_{nm} + o(1)\} \quad \text{as } k \to \infty. \tag{2.4}$$

Here $\alpha_{nm} = [\Lambda'_{nm}]^+_-$ is the discontinuous change in slope at the crest. This analysis shows explicitly that the discontinuity in slope at the Λ-crest leads to the Fourier transform behaving as k^{-2} as $kl_n \to \infty$. In (2.4) $\tilde{\Lambda}_{nm}$ is written as a magnitude multiplied by a phase factor, with a phase ϕ_{nm} that is determined by the position of the crest, $\phi_{nm} = kx_{nm}$. We assume that, at sufficiently high wavenumbers, $\tilde{\zeta}_s$ is much smaller than the contribution from the Λ-crests, so that the spectrum is dominated by the contribution from the Λ-crests.

In the following calculation, we shall also need a qualitative understanding of the behaviour of $\tilde{\Lambda}_{nm}$ at small k. There is no variation of the Λ-crest on lengthscales greater than l_n and so $\tilde{\Lambda} \sim 0$ for $kl_n \lesssim 1$. Hence $\tilde{\Lambda}_{nm}$ first increases with kl_n from zero, reaches a maximum when $kl_n = O(1)$, and then decays as $(kl_n)^{-2}$ at larger values of kl_n. This behaviour will be approximated here by

$$\tilde{\Lambda}_{nm}(k, l_n, x_{nm}) = \frac{1}{2\pi} l_n \mathrm{e}^{\mathrm{i}\phi_{nm}} \frac{1}{(kl_n)^2}\alpha_{nm}\mathrm{H}(kl_n - 1), \tag{2.5}$$

where H is the Heaviside step function.

2.2. *Spectrum of a set of Λ-crests*

The next step is to use the Fourier transform of a single Λ-crest to calculate the one-dimensional wavenumber spectrum. For illustration, consider first Λ-crests with discrete scales, l_n (a continuous range of scales is considered in §2.4).

At high wavenumbers, the Fourier transform of the wave surface is dominated by the Fourier transform of the Λ-crests and so on using (2.1) and (2.5), we find

$$\tilde{\zeta}(k) = \frac{1}{2\pi k^2}\sum_{nm} \alpha_{nm}\beta_{nm}\mathrm{H}(kl_n - 1)\mathrm{e}^{\mathrm{i}\phi_{nm}(k)} + o(k^{-2}), \tag{2.6}$$

where $\beta_{nm} = a_{nm}/l_n$ is the slope of the nmth wave. Hence, to begin calculating the spectrum, write

$$|\tilde{\zeta}(k)|^2 = \left(\frac{1}{2\pi k^2}\right)^2 \left| \left\{\sum_n \mathrm{H}(kl_n - 1)\sum_m (\alpha_{nm}\beta_{nm})\mathrm{e}^{\mathrm{i}\phi_{nm}(k)}\right\} \right.$$
$$\left. \times \left\{\sum_p \mathrm{H}(kl_p - 1)\sum_q (\alpha_{pq}\beta_{pq})\mathrm{e}^{\mathrm{i}\phi_{pq}(k)}\right\}^* \right|. \tag{2.7}$$

There are three random elements in this expression, namely the positions, x_{nm}, of the crests (and hence the phases ϕ_{nm}), the slope discontinuities at the Λ-crests, α_{nm}, and the overall slopes of the waves, β_{nm}. And so to form $\Psi_1(k)$ requires averaging over these random processes, which are assumed to be independent and uncorrelated.

Experimental data (Shen *et al.* 1994) show no coherence in the positions of the Λ-crests. Hence assume the x_{nm} are uncorrelated and uniformly distributed, so that the ϕ_{nm} are uniformly distributed between 0 and 2π, which implies that

$$\overline{|\mathrm{e}^{\mathrm{i}\phi_{nm}}\mathrm{e}^{-\mathrm{i}\phi_{pq}}|} = \delta_{np}\delta_{mq}. \tag{2.8}$$

As argued in §1.1, the geometry of breaking waves is on average self similar, hence α_{nm} and β_{nm} average to well-defined values that are independent of l_n, namely α_Λ and β_Λ which are defined by

$$\alpha_\Lambda^2 \beta_\Lambda^2 = \overline{\alpha_{nm}^2 \beta_{nm}^2}. \tag{2.9}$$

With these averages performed and using (2.2), the wavenumber spectrum becomes

$$\Psi_1(k) = \frac{(\alpha_\Lambda \beta_\Lambda)^2}{L_x k^4} \sum_n \sum_m \mathrm{H}(kl_n - 1) = \frac{(\alpha_\Lambda \beta_\Lambda)^2}{k^4} \sum_n M_n \mathrm{H}(kl_n - 1), \tag{2.10}$$

where M_n is the expected number of Λ-crests of size l_n per unit length of wave record (i.e. the total number in the record is $L_x M_n$). For given wavenumber k, contributions to the spectrum arise only from Λ-crests that can be resolved by the wavenumber of size k, i.e. Λ-crests with $kl_n \geqslant 1$. This behaviour arises mathematically through the Heaviside step functions in (2.10) and means that the sum over n has a finite number of terms, $P(k)$, defined by $l_{P(k)} \geqslant k^{-1} > l_{P(k)+1}$. Denote the total number of Λ-crests resolved at wavenumber k, i.e. the total number with scales greater that k^{-1}, by $M_1^>(k)$, so that

$$M_1^>(k) = \sum_n^{P(k)} M_n. \tag{2.11}$$

The wavenumber spectrum is then

$$\Psi_1(k) = (\alpha_\Lambda \beta_\Lambda)^2 \frac{1}{k^4} M_1^>(k). \tag{2.12}$$

Hence, if $M_1^>(k)$ is independent of k then the distribution of sharp-crested one-dimensional waves has a wavenumber spectrum that varies as k^{-4}. The coefficient multiplying this power law depends on the number of resolved breaking waves per unit length, $M_1^>(k)$, and the average wave shape, through α_Λ, the jump in slope at the crest, and β_Λ, the overall slope of the breaking waves. But $M_1^>(k)$ may vary with k and possibly change the behaviour of the spectrum. This possibility is explored in the next section.

2.3. *Spectrum of a discrete distribution of self-similar Λ-crests*

The next step is to examine how the spectrum varies with k when the surface has a scale-invariant distribution of Λ-crests. As shown in §1.2, when the surface waves are scale invariant the expected number of Λ-crests of scale l_n per unit length has a power-law dependence on l_n, namely

$$M_n = M_0 \left(l_0/l_n\right)^{D_1}, \tag{2.13}$$

where M_0 is the number of Λ-crests of outer scale l_0. The exponent D_1 parameterizes the distribution of one-dimensional Λ-crests with their lengthscale l_n.

The variation in M_n given by (2.13) implies that the wavenumber spectrum (2.10) becomes

$$\Psi_1(k) = \frac{(\alpha_\Lambda \beta_\Lambda)^2}{k^4} \sum_n M_0 \left(\frac{l_0}{l_n}\right)^{D_1} \mathrm{H}(kl_n - 1). \tag{2.14}$$

As in §2.2, the Heaviside functions in (2.14) mean that the sum is finite with $P(k)$ terms. The key new feature of (2.14) is that as k increases so does $P(k)$, which can lead to the wavenumber spectrum varying as a power law different from k^{-4}.

This feature is illustrated in figure 2. Each of the four curves shown on figure 2(*a*) corresponds to the spectrum (multiplied by k^4) given by a single term in the sum over n in (2.14) when $D_1 = 1$, and when $\alpha_\Lambda = \beta_\Lambda = 1$. Hence the first curve corresponds to $n = 0$ and results from 4 Λ-crests of scale 1, the second results from 32 Λ-crests of scale $\frac{1}{8}$ ($n = 3$), the third results from 256 Λ-crests of scale $\frac{1}{64}$ ($n = 6$) and the fourth results from 2048 Λ-crests of scale $\frac{1}{512}$ ($n = 9$). Hence for this illustration we have chosen $l_n/l_0 = 1/2^n$ and $M_0 = 4$ so that $M_n = 2^{n+2}$. The total wavenumber spectrum for $D_1 = 1$, which is also shown as a straight line on the figure, is the sum of each of these curves (plus intermediate terms in the sum that for clarity have been omitted from the figure). On the logarithmic axes, each curve is small for $kl_n \lesssim 1$, but rapidly increases to a constant value when $kl_n \gtrsim 1$, i.e. when the Λ-crests are resolved. The constant value attained when $kl_n \gg 1$ scales with the number of Λ-crests and so increases as l_n decreases. Hence, if the total spectrum is $\Psi_1(k)$, then $k^4\Psi_1(k) \sim k$ when $D_1 = 1$ because more Λ-crests are resolved at small scales.

Figure 2(*b*) shows similar curves when $D_1 = -1$, and when $\alpha_\Lambda = \beta_\Lambda = 1$: the first curve correponds to $n = 3$ and results from 256 Λ-crests of scale $\frac{1}{8}$, the second results from 32 Λ-crests of scale $\frac{1}{64}$ ($n = 6$), the third results from 4 Λ-crests of scale $\frac{1}{512}$ ($n = 9$). Hence for this illustration we have chosen $l_n/l_0 = 1/2^n$ and $M_0 = 2048$ so that $M_n = 2^{11-n}$. The contributions to the spectrum decrease with n, so that the total spectrum obtained by summing these (and other) terms is dominated by the first, and largest, term. This largest term varies like the spectrum of a single Λ-crest and hence $k^4\Psi(k)$ is constant at high wavenumbers and scales on the number of largest Λ-crests.

These effects are demonstrated analytically in the next section when a collection of Λ-crests with a continuous range of sizes is considered.

2.4. *Spectrum of a continuous distribution of self-similar Λ-crests*

In the analysis so far we have considered a set of Λ-crests of discrete scales, l_n. Waves on the ocean have a continuous range of scales, and so do the breaking waves. Hence the expression for the one-dimensional wavenumber spectrum (2.10) is now generalized to a continuous distribution of Λ-crests. In this case M_n, the number of Λ-crests of scale l_n, is replaced by a *number density*, namely

$$\mathrm{d}M_1 = M_1(l_1)\mathrm{d}l_1, \tag{2.15}$$

which represents the expected number of Λ-crests with scales in the range l_1 to $l_1 + \mathrm{d}l_1$ per unit length along the slice through the wave field. As discussed in §1.2, for a scale-invariant sea surface the variation of the number density with scale can only be as a power law as in the discrete case. For convenience later the power law is written

$$M_1(l_1)\mathrm{d}l_1 = \frac{M_0}{l_0}\left(\frac{l_0}{l_1}\right)^{D_1+1}\mathrm{d}l_1, \tag{2.16}$$

which holds in the scale-invariant range, where $l_1 \leqslant l_0$. The number of Λ-crests resolved at wavenumber k, denoted by $M_1^{>}(k)$, is given by

$$M_1^{>}(k) = \int_{k^{-1}}^{l_0} M_1(l_1)\mathrm{d}l_1 = \begin{cases} \left(M_0/D_1\right)\left\{(kl_0)^{D_1} - 1\right\}, & D_1 \neq 0 \\ M_0 \ln(kl_0), & D_1 = 0, \end{cases} \tag{2.17}$$

so that M_0 has a meaning analogous to that in the discrete case (2.13), i.e. the number of Λ-crests with scales larger than l_0.

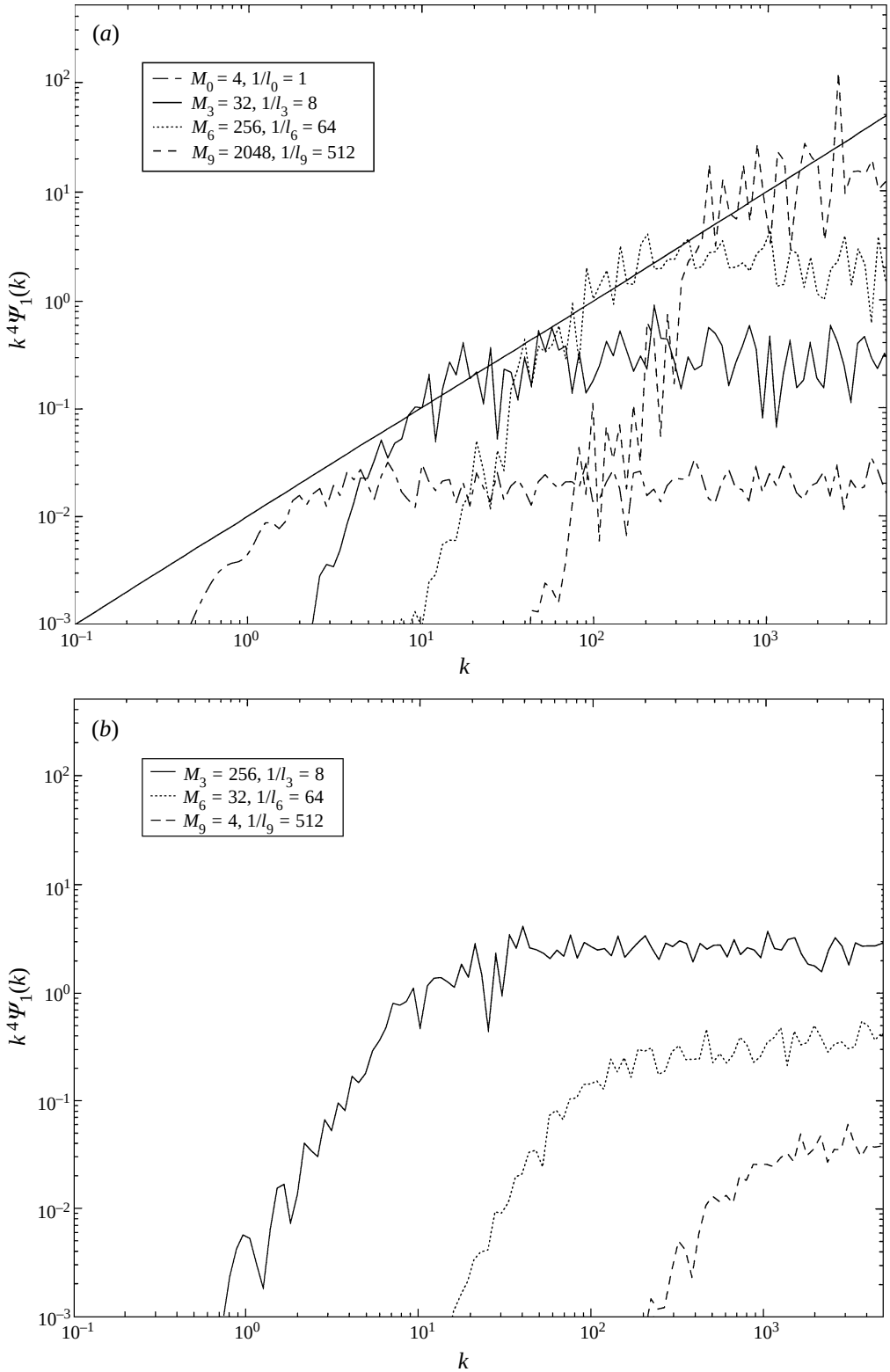

FIGURE 2. Contributions to the spectrum: (*a*) $D = 1$, (*b*) $D = -1$.

The discrete sum over M_n in the expression for the spectrum (2.10) becomes an integral when there is a continuous distribution of Λ-crests, so that the one-dimensional wavenumber spectrum becomes

$$\Psi_1(k) = \frac{(\alpha_\Lambda \beta_\Lambda)^2}{k^4} \int_0^{l_0} M_1(l_1) \mathrm{H}(kl_1 - 1) \mathrm{d}l_1 = \frac{(\alpha_\Lambda \beta_\Lambda)^2}{k^4} M_1^{>}(k), \tag{2.18}$$

because the Heaviside step function means that the lower limit of integration is $l_1 = k^{-1}$, i.e. only resolved Λ-crests with $l_1 \geqslant k^{-1}$ are included. Equation (2.17) can be used in this expression to compute the one-dimensional spectrum, which becomes

$$\Psi_1(k) = \begin{cases} \dfrac{(\alpha_\Lambda \beta_\Lambda)^2}{D_1} \dfrac{M_0}{k^4} \left\{ (kl_0)^{D_1} - 1 \right\}, & D_1 \neq 0 \\ \dfrac{(\alpha_\Lambda \beta_\Lambda)^2}{D_1} \dfrac{M_0}{k^4} \ln(kl_0), & D_1 = 0. \end{cases} \tag{2.19}$$

There are three cases: $D_1 > 0$, $D_1 < 0$, and $D_1 = 0$. They can be understood by examining the ratio of the number of Λ-crests with sizes between l_1 and $l_1 + \mathrm{d}l_1$ to the number with sizes between sl_1 and $s(l_1 + \mathrm{d}l_1)$, namely

$$\frac{M_1(l_1)\mathrm{d}l_1}{M_1(sl_1)\mathrm{d}(sl_1)} = s^{D_1}, \tag{2.20}$$

which, when $s > 1$, measures the ratio of the number of small crests to the number of large crests.

First, suppose that $D_1 > 0$, so that (2.20) is greater than 1 and there are more small Λ-crests than large. Equation (2.19) is then dominated by the first term in the curly bracket and

$$\Psi_1(k) \sim \frac{(\alpha_\Lambda \beta_\Lambda)^2}{D_1} M_0 \frac{1}{k^4} (kl_0)^{D_1} \quad \text{when } kl_0 \gg 1, \tag{2.21}$$

which decays as k^{-4+D_1} (cf. figure 2*a*). The exponent is changed from -4 because, as the wavenumber increases, smaller Λ-crests are resolved, and, because the number of small Λ-crests is greater than the number of large Λ-crests, there is more energy associated with the small scales and the spectrum decays more slowly than k^{-4}.

Secondly, suppose that $D_1 < 0$, then (2.20) is less than 1 and so there are fewer small crests than large. The second term in the bracket of (2.19) is then largest, because $(kl_0)^{D_1} \to 0$ when $kl_0 \gg 1$. Hence

$$\Psi_1(k) \sim \frac{(\alpha_\Lambda \beta_\Lambda)^2}{|D_1|} M_0 \frac{1}{k^4} \quad \text{when } kl_0 \gg 1, \tag{2.22}$$

which decays as k^{-4} (cf. figure 2*b*). In this case, although there are small-scale Λ-crests, they are fewer in number than the large Λ-crests, and so the small-scale Λ-crests contribute negligible energy to the spectrum and the spectrum shows the signature of only the large Λ-crests. So in this case, the high-wavenumber part of the spectrum contains information about only the largest breaking waves.

The third case of $D_1 = 0$ is the limiting case in the kinematics when (2.20) equals 1 and the number of Λ-crests is independent of scale and so there are just enough small-scale Λ-crests to contribute to the spectrum. Hence the spectrum decays as $k^{-4} \ln(k/k_0)$, which is just a little slower than k^{-4}.

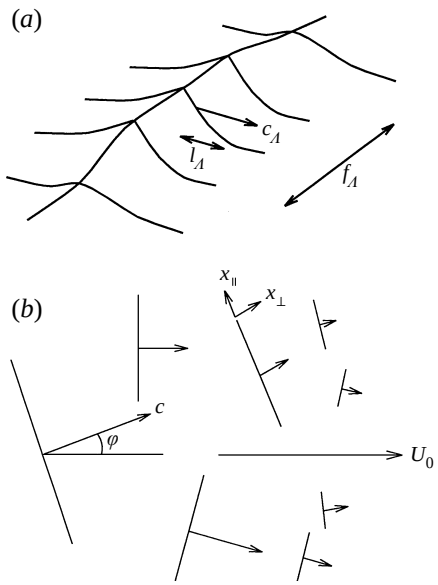

FIGURE 3. Representation of the two-dimensional sea surface as a collection of breaking-wave fronts with discontinuous slopes at their crests. (*a*) A single breaking-wave front; (*b*) a collection of breaking-wave fronts.

2.5. *Spectrum of two-dimensional breaking waves*

Thus far we have considered only a one-dimensional cut through the sea surface and so we now consider the full two-dimensional sea surface. Take the x-axis ($\theta = 0$) along the wind direction. Then in two dimensions the breaking waves are modelled as breaking-wave fronts that consist of straight-line segments of sharp-crested waves, with cross-sections like the one-dimensional Λ-crests and with smooth modulation, Υ, along the length of the crest, i.e. $\Lambda(x, y) = \Lambda(x_\perp)\Upsilon(x_\parallel)$, where $x_\perp$ and $x_\parallel$ are the distances perpendicular and parallel to the breaking front (see figure 3). The lengthscale along a breaking front is f_Λ, so that $\Upsilon(x_\parallel) \sim 1$ when $x_\parallel \lesssim f_\Lambda$ and $\Upsilon(x_\parallel) \to 0$ when $x_\parallel \gg f_\Lambda$. For definiteness and mathematical convenience, we take $\Upsilon(x_\parallel) = \exp(-x_\parallel^2/f_\Lambda^2)$; the form of the results remains the same for other choices. The sea-surface elevation, $\zeta(x, y)$ is modelled as a collection of these two-dimensional Λ-crests, located randomly, and propagating at angle φ to the x-axis with probability distribution $\Theta(\varphi)$ (see figure 3*b*).

The two-dimensional wavenumber spectrum, $\Psi(\boldsymbol{k})$ of such waves is related to the two-dimensional Fourier transform of the surface elevation, $\tilde{\zeta}(\boldsymbol{k})$, by

$$\Psi(\boldsymbol{k}) = \frac{(2\pi)^4}{L_x L_y}\overline{|\tilde{\zeta}(\boldsymbol{k})|^2}, \tag{2.23}$$

where the overbar denotes averaging over realizations and averaging over x between 0 and L_x and y between 0 and L_y.

The sea-surface elevation, $\zeta(x, y)$, is written as a sum of Λ-crests, and calculation of the spectrum begins with calculating its Fourier transform, $\zeta(\boldsymbol{k})$. The Fourier transform of a single two-dimensional Λ-crest is

$$\tilde{\Lambda}(\boldsymbol{k}) = \tilde{\Lambda}(k_\perp)\tilde{\Upsilon}(k_\parallel), \tag{2.24}$$

where $k_\perp = k\cos(\theta - \varphi)$ and $k_\parallel = k\sin(\theta - \varphi)$ are the components of the wavenumber,

$\boldsymbol{k}$, perpendicular and parallel to the breaking front. $\tilde{\Lambda}$ is the same as in (2.5) and for the Gaussian smoothing $\tilde{\Upsilon} = (1/2\pi^{1/2}) f_\Lambda \exp(-\frac{1}{4} f_\Lambda^2 k_\parallel{}^2)$.

The calculation then proceeds following the same methodology as developed in §2 for the one-dimensional case. The square of the sum of the Fourier transforms of all the Λ-crests is formed and averaged over the positions of the centres of the Λ-crests; this procedure yields

$$\frac{1}{L_x L_y} \overline{|\tilde{\zeta}(\boldsymbol{k})|^2} = \int_0^{l_0} a_\Lambda^2 \, |\tilde{\Lambda}(k_\perp)|^2 \, |\Upsilon(k_\parallel)|^2 \, M(l_\Lambda) \, \mathrm{d}l_\Lambda, \tag{2.25}$$

where a_Λ is the amplitude of the Λ-crest and $M(l_\Lambda)\mathrm{d}l_\Lambda$ is the number of breaking-wave fronts with sizes in the range l_Λ to $l_\Lambda + \mathrm{d}l_\Lambda$ per *unit area* (in the one-dimensional case it was the number per *unit length* that was relevent).

The final step is to take averages over the directions of propagation of the breaking-wave front, φ. This part of the calculation becomes more transparent if we note that

$$|\Upsilon(k_\parallel)|^2 = \frac{1}{4\pi} f_\Lambda^2 \exp(-\tfrac{1}{2} f_\Lambda^2 k_\parallel{}^2) \sim \frac{1}{2(2\pi)^{1/2}} \delta(k_\parallel) f_\Lambda \quad \text{for } f_\Lambda k_\parallel \gg 1. \tag{2.26}$$

Here $\delta(k_\parallel)$ is the Dirac delta function, which ensures that for long breaking-wave fronts (large f_Λ) $k_\parallel$ must be zero so that the wavenumber vector is perpendicular to the breaking-wave front.

Hence we now average over the directions of propagation, φ, which have probability density function $\Theta(\varphi)$. Then the two-dimensional wavenumber spectrum is given by

$$\begin{aligned} \Psi(\boldsymbol{k}) &= (2\pi)^4 \int_{-\pi}^{\pi} \left\{ \int_0^{l_0} a_\Lambda^2 \, |\tilde{\Lambda}(k_\perp)|^2 \, \frac{1}{2(2\pi)^{1/2}} \delta(k_\parallel) f_\Lambda \, M(l_\Lambda) \, \mathrm{d}l_\Lambda \right\} \Theta(\varphi) \mathrm{d}\varphi \\ &= (2\pi)^4 \int_0^{l_0} a_\Lambda^2 \, |\tilde{\Lambda}(k)|^2 \, \frac{1}{2(2\pi)^{1/2}} f_\Lambda \, M(l_\Lambda) \frac{1}{k} \, \mathrm{d}l_\Lambda. \end{aligned} \tag{2.27}$$

On integration over the propagation angles, the delta function, $\delta(k_\parallel)$, picks out the wavenumber vectors with $k_\parallel = 0$ and leads to a multiplicative factor of $1/k$, which is important because it changes the power-law variation of $\Psi(\boldsymbol{k})$ with k. Different choices for the smoothing, Υ, give the same variation with k and θ, but change the numerical coefficient in (2.27).

The final form of the wavenumber spectrum can be computed using the form of $\tilde{\Lambda}(k)$ given in (2.5), which shows that

$$\Psi(\boldsymbol{k}) = \tfrac{1}{2}(2\pi)^{3/2} \alpha_\Lambda^2 \beta_\Lambda^2 \Theta(\theta) \frac{1}{k^5} \int_0^{l_0} F(l_\Lambda) \mathrm{H}(k l_\Lambda - 1) \, \mathrm{d}l_\Lambda, \tag{2.28}$$

where by definition $F(l_\Lambda)\mathrm{d}l_\Lambda = f_\Lambda M(l_\Lambda)\mathrm{d}l_\Lambda$ is the total length of all breaking-wave fronts with scales between l_Λ and $l_\Lambda + \mathrm{d}l_\Lambda$ per unit area of sea surface. This total length can vary with l_Λ and hence plays the role that $M_1(l_1)$ plays in the one-dimensional calculation.

The arguments of §1.2 are again invoked to show that $F(l_\Lambda)$ varies with l_Λ as a power law, namely

$$F(l_\Lambda)\mathrm{d}l_\Lambda = \frac{F_0}{l_0} \left(\frac{l_0}{l_\Lambda} \right)^{D+1} \mathrm{d}l_\Lambda. \tag{2.29}$$

The two-dimensional wavenumber spectrum is then

$$\Psi(\boldsymbol{k}) = \begin{cases} \frac{1}{2}(2\pi)^{3/2}(\alpha_\Lambda \beta_\Lambda)^2 \dfrac{1}{D}\dfrac{F_0}{k^5}\Theta(\theta)\left\{(kl_0)^D - 1\right\}, & D \neq 0 \\ \\ \frac{1}{2}(2\pi)^{3/2}(\alpha_\Lambda \beta_\Lambda)^2 \dfrac{F_0}{k^5}\Theta(\theta)\ln(kl_0), & D = 0. \end{cases} \tag{2.30}$$

The two-dimensional wavenumber spectrum of a distribution of breaking-wave fronts with discontinuous slopes aligned in random directions therefore decays as k^{-5}. This is faster than the spectrum of the one-dimensional elevation which decays as k^{-4}. The faster decay in the two-dimensional spectrum is because the two-dimensional surface is made up of line singularities of characteristic length f_Λ. When viewed on lengthscales greater than f_Λ the surface is then fully two-dimensional, because the Λ-crests vary both across and along the crest. But when the surface is viewed on lengthscales smaller than f_Λ the waves are predominantly one-dimensional because the Λ-crests vary only across the crests. This one-dimensional character at high wavenumbers means that there is less energy at high wavenumbers and therefore the spectrum decays faster.

2.6. *Relationship between $\Psi_1(k)$ and $\Psi(\boldsymbol{k})$*

It is interesting to relate the spectra obtained in one- and two-dimensional cases. To do this requires relating the number density (per unit area) of the two-dimensional Λ-crests, $M(l)\mathrm{d}l$, to the number density (per unit length) along a straight-line cut through the sea surface, $M_1(l_1)\mathrm{d}l_1$. For simplicity, we begin with the spectrum of surface displacement along the x-axis.

A Λ-crest of scale l_Λ moving at angle φ to the x-axis has a cross-sectional scale along the x-axis of $l_1 = l_\Lambda \cos\varphi$, hence

$$M(l_\Lambda)\mathrm{d}l_\Lambda = M\left(\frac{l_1}{\cos\varphi}\right)\frac{\mathrm{d}l_1}{\cos\varphi}. \tag{2.31}$$

When the Λ-crests are uniformly distributed in the sampling area $L_x L_y$, only a fraction $f_\Lambda \cos\varphi / L_y$ cut the x-axis. Hence $M_1 \mathrm{d}l_1$, the average number of Λ-crests with scales in the range l_1 to $l_1 + \mathrm{d}l_1$ that are detected per unit length along the x-axis, is given by

$$M_1(l_1)\mathrm{d}l_1 = \int_{-\pi}^{\pi}\left\{M\left(\frac{l_1}{\cos\varphi}\right) f_\Lambda \cos\varphi \frac{\mathrm{d}l_1}{\cos\varphi}\right\}\Theta(\varphi)\,\mathrm{d}\varphi. \tag{2.32}$$

Recall that by definition $F(l_\Lambda) = f_\Lambda M(l_\Lambda)$, which is written as a power of l_Λ in (2.29), so that

$$M_1(l_1)\mathrm{d}l_1 = \frac{F_0}{l_0}\left(\frac{l_0}{l_1}\right)^{D+1}\left\{\int_{-\pi}^{\pi}(\cos\varphi)^{D+1}\Theta(\varphi)\,\mathrm{d}\varphi\right\}\mathrm{d}l_1. \tag{2.33}$$

Comparison of this expression with the definition (2.16) shows that

$$D_1 = D, \tag{2.34}$$

and

$$M_0 = F_0\int_{-\pi}^{\pi}(\cos\varphi)^{D+1}\Theta(\varphi)\,\mathrm{d}\varphi. \tag{2.35}$$

Hence, with these results, given the value of D, $\Psi_1(k)$ can be calculated using (2.19).

When the line through the sea surface is at angle θ_0 to the x-axis, the only difference is that the probability density function shifts around and becomes $\Theta(\varphi - \theta_0)$, so that

$$M_0 = F_0 \int_{-\pi}^{\pi} (\cos\varphi)^{D+1} \Theta(\varphi - \theta_0)\, \mathrm{d}\varphi. \tag{2.36}$$

Hence the one-dimensional spectrum has the same power-law variation with k for all angles, but the coefficient multiplying this power law varies with the angle.

3. Dynamical determination of D

As explained in §1.2 the sea surface is scale invariant if both the geometry of individual waves is scale invariant and if the dynamical processes that determine the distribution of these breaking waves is scale invariant. When the dynamical processes are scale invariant, the total length of breaking-wave fronts with scales in the range l_Λ to $l_\Lambda + \mathrm{d}l_\Lambda$ varies as a power law (2.29). The exponent D cannot be determined by kinematical ideas; dynamical arguments need to be invoked. We now follow an approach suggested by Phillips (1985) and develop a scaling for the dynamical balance in the equilibrium range. This dynamical balance enables D to be fixed.

3.1. *Rate of spectral action dissipation*

Evolution of the wavenumber spectrum can be conveniently phrased in terms of the spectral wave-action density, $N(\boldsymbol{k})$, which is conserved in wave–current interactions (e.g. Phillips 1977, p. 179). Equilibrium in the high-wavenumber part of the spectrum means that $\mathrm{D}N(\boldsymbol{k})/\mathrm{D}t$, the rate of change of the spectral density of wave action at wavenumber $\boldsymbol{k}$, is much smaller than the sources and sinks of wave action at that wavenumber. Hence the sources and sinks balance, and can be written

$$S_w(\boldsymbol{k}) - \nabla_{\boldsymbol{k}} \cdot \boldsymbol{T}(\boldsymbol{k}) - \varepsilon_N(\boldsymbol{k}) = 0, \tag{3.1}$$

where $S_w(\boldsymbol{k})$ is the wind input of wave action, $\boldsymbol{T}(\boldsymbol{k})$ is the flux of wave action through wavenumber $\boldsymbol{k}$ by wave–wave interactions, and $\varepsilon_N(\boldsymbol{k})$ is the rate of dissipation of wave action.

This tripartite balance can be used to estimate $\varepsilon_N(\boldsymbol{k})$ when the dynamical balance in the equilibrium range is scale invariant. The reasoning for $M(l_\Lambda)$ being proportional to a power of l_Λ given in §1.2 can be applied to each term in (3.1), which shows that these terms are proportional to $(kl_0)^p$ for some p. But the three terms in (3.1) then balance over a range of k only if each has the same exponent p, which means that the three terms are proportional to one another.

The rate of spectral action dissipation can now be estimated by balancing with the nonlinear flux divergence, so that

$$\varepsilon_N(\boldsymbol{k}) = \gamma \nabla_{\boldsymbol{k}} \cdot \boldsymbol{T}(\boldsymbol{k}), \tag{3.2}$$

where γ is the coefficent of proportionality, which is independent of k, but may depend on other parameters such as U_0/c_p.

The next step is to estimate the magnitude of the nonlinear flux divergence. For gravity waves of low slope, $ak \ll 1$, nonlinear interactions are very weak and energy exchange occurs between four waves; the three-wave interaction is prohibited for gravity waves that follow the linear dispersion relation (see e.g. Phillips 1977, p. 82). Hence the rate of growth of the amplitude of the Fourier component of wavenumber $\boldsymbol{k}$ is proportional to the product of the amplitudes of the other three waves. Now $\Psi(\boldsymbol{k})$ is proportional to the square of the wave amplitude, and the rate of change

of $\Psi(\boldsymbol{k})$ by very weak nonlinear interactions is proportional to the product of the spectral-energy density of the three other interacting components. In the equilibrium range there is no wavenumber scale other than $\boldsymbol{k}$, and very weak nonlinear wave–wave interactions are predominantly local in wavenumber space (see Phillips 1985). Hence the rate of change of action density at wavenumber $\boldsymbol{k}$ due to wave–wave interactions scales on $\Psi^3(\boldsymbol{k})$ (see Kitaigorodskii 1983).

According to our model, the equilibrium range is dominated by sharp-crested breaking waves, each of which is composed of many Fourier components all instantaneously travelling at the same phase speed. Hence these waves are intrinsically nonlinear and the classical theory of wave–wave interaction is not adequate. But we expect interactions between Λ-crests to remain weak because the overall slope of breaking waves is smaller than 1 (typically $\frac{1}{3}$ according to Bonmarin 1989); stronger nonlinear interactions might occur within a single Λ-crest, but they are associated with actual overturning of a breaking wave. Hence, the weakly nonlinear framework remains appropriate and we suppose here that nonlinear interaction between Λ-crests involves $q+1$ Fourier modes, for some $q > 1$. Most of the energy associated with a Λ-crest of scale l is contained in the Fourier mode with wavenumber l^{-1} that determines the propagation speed of the Λ-crest. Hence we might expect the classical four-wave interaction to be dominant so that q is close to 3, the value for very weak interactions. It is then consistent to suppose that, like the classical four-wave interaction, the interactions between Λ-crests remain local in wavenumber space. The magnitude of the nonlinear flux divergence can then be estimated using similar reasoning as used above, so that

$$\nabla_{\boldsymbol{k}} \cdot \boldsymbol{T}(\boldsymbol{k}) \propto \Psi^q(\boldsymbol{k}). \tag{3.3}$$

If these nonlinear interactions are, at leading order, unaffected by the wind then, in addition to $\Psi(\boldsymbol{k})$, they can depend only on $\boldsymbol{k}$ and g. Hence, on dimensional grounds, the nonlinear-flux divergence can be estimated to be

$$\nabla_{\boldsymbol{k}} \cdot \boldsymbol{T}(\boldsymbol{k}) \sim \mathrm{g}k^{-4}\{k^4\Psi(\boldsymbol{k})\}^q = \mathrm{g}k^{-4}B^q(\boldsymbol{k}), \tag{3.4}$$

where, following Phillips (1985), the saturation spectrum is defined by $B(\boldsymbol{k}) = k^4\Psi(\boldsymbol{k})$. When $q = 3$ this estimate agrees with the scaling given by Kitaigorodskii (1983) based on his estimate of the 'collision integral' for a very weakly interacting random set of gravity waves of low slope.

This estimate of the nonlinear-flux divergence, together with (3.2), suggests that the spectral action dissipation rate scales as

$$\varepsilon_N(\boldsymbol{k}) = \gamma \mathrm{g}k^{-4}B^q(\boldsymbol{k}). \tag{3.5}$$

This method of estimating the rate of dissipation of wave action avoids using a phase speed or frequency of the Fourier modes that comprise the Λ-crests. This is important because the action density at wavenumber $\boldsymbol{k}$ has contributions from Λ-crests of many different scales, as does the wavenumber spectrum, and so it is not clear how such quantities can be even defined; they are certainly *not* given by the relations for freely moving linear waves.

The final step in estimating $\varepsilon_N(\boldsymbol{k})$ is to use the saturation spectrum derived from the two-dimensional wavenumber spectrum of a collection of sharp-crested breaking waves given in (2.30). When $D > 0$, which will be confirmed later by this calculation, (2.30) shows that when $kl_0 \gg 1$ the saturation spectrum is

$$B(\boldsymbol{k}) = \tfrac{1}{2}(2\pi)^{3/2}(\alpha_\Lambda\beta_\Lambda)^2\frac{1}{D}F_0 l_0\,\Theta(\theta)\,(kl_0)^{D-1}. \tag{3.6}$$

The rate of spectral action dissipation is therefore

$$\varepsilon_N(\boldsymbol{k})\mathrm{d}\boldsymbol{k} = \gamma' \mathrm{g} k^{-4} \left\{ F_0 l_0 \, \Theta(\theta) \, (k l_0)^{(D-1)} \right\}^q \, k \, \mathrm{d}k \, \mathrm{d}\theta, \tag{3.7}$$

where $\gamma' = \gamma \{ \frac{1}{2} (2\pi)^{3/2} (\alpha_\Lambda \beta_\Lambda)^2 \frac{1}{D} \}^q$ is a constant.

3.2. *Rate of mechanical energy dissipation*

As explained in §1.1, an estimate of the energy dissipation rate of a continuously breaking wave front has been developed by Duncan (1981) by using simple mechanical ideas to relate the energy dissipated to the size, l_Λ, of the wave. Melville (1994) has suggested that the scaling remains valid for unsteady breakers. Hence, if $F(l_\Lambda)\mathrm{d}l_\Lambda$ is the expected length of breaking fronts with scales in the range l_Λ to $l_\Lambda + \mathrm{d}l_\Lambda$ per unit area of sea surface, then the rate of energy dissipation per unit area of sea surface is

$$\varepsilon_E(l_\Lambda, \theta)\mathrm{d}\boldsymbol{l}_\Lambda = b \mathrm{g} c_\Lambda l_\Lambda^2 \, F(l_\Lambda)\mathrm{d}l_\Lambda \, \Theta(\theta)\mathrm{d}\theta, \tag{3.8}$$

where $b \approx 0.044 \pm 0.08$ is a coefficient determined by Melville's (1994) analysis of Duncan's (1981) data; its value may be up to a factor 10 smaller for unsteady breakers (Melville 1994). Since Λ-crests move coherently at a speed $c_\Lambda(l_\Lambda)$ they have a frequency, $\sigma_\Lambda(l_\Lambda)$, defined by $\sigma_\Lambda = c_\Lambda / l_\Lambda$. Hence the rate of dissipation of action density due to the breaking of Λ-crests is

$$\varepsilon_N(l_\Lambda, \theta)\mathrm{d}\boldsymbol{l}_\Lambda = \frac{1}{\sigma_\Lambda} \varepsilon_E(l_\Lambda, \theta)\mathrm{d}\boldsymbol{l}_\Lambda = b \mathrm{g} l_\Lambda^3 \, F(l_\Lambda)\mathrm{d}l_\Lambda \, \Theta(\theta)\mathrm{d}\theta. \tag{3.9}$$

This provides a second estimate of the rate of action dissipation, which, on using (2.29), depends on the exponent D.

3.3. *Determination of D*

The two estimates of the dissipation rate found above, (3.7) and (3.9), must be consistent, which is now used to determine the exponent D. Care must be used however because $\varepsilon_N(\boldsymbol{k})\mathrm{d}\boldsymbol{k}$ is the rate of action dissipation from a small band of wavenumbers, whereas $\varepsilon_N(\boldsymbol{l}_\Lambda)\mathrm{d}\boldsymbol{l}_\Lambda$ is the dissipation rate from breaking waves from a small band of scales. The two estimates cannot be simply equated because breaking is associated with particular Λ-crests in physical space and each Λ-crest consists of a wide range of Fourier components. Hence, at a particular value of k, $\varepsilon_N(\boldsymbol{k})\mathrm{d}\boldsymbol{k}$ contains contributions from Λ-crests of a range of sizes. This argument means that there is no one-to-one relationship between l_Λ and k or between $\varepsilon_N(\boldsymbol{l}_\Lambda)\mathrm{d}\boldsymbol{l}_\Lambda$ and $\varepsilon_N(\boldsymbol{k})\mathrm{d}\boldsymbol{k}$.

Equivalence between the two estimates of dissipation rate can be enforced on recognizing that a Λ-crest of scale l_Λ has Fourier components only in the range $k \geqslant l_\Lambda^{-1}$. Hence the dissipation in wavenumber scales in the range l_Λ^{-1} to infinity is associated only with Λ-crests with physical scales in the range 0 to l_Λ; hence

$$\int_0^{l_\Lambda} \int_0^{2\pi} \varepsilon_N(\boldsymbol{l}_\Lambda)\mathrm{d}\boldsymbol{l}_\Lambda = \int_{l_\Lambda^{-1}}^{\infty} \int_0^{2\pi} \varepsilon_N(\boldsymbol{k})\mathrm{d}\boldsymbol{k}. \tag{3.10}$$

The integrals can easily be performed and the results vary with l_Λ. Hence, the resulting equation has powers of l_Λ on each side. The powers, and hence the two estimates of the dissipation rate, are consistent if and only if

$$3 - D = 2 - q(D - 1). \tag{3.11}$$

Hence, provided $q \neq 1$ (which is satisfied provided the nonliner interactions *are* nonlinear), this equation is satisfied for one and only one value of D, namely

$$D = 1. \tag{3.12}$$

This is a striking result. It is striking because it was by no means obvious that the kinematics would be consistent with the dynamics. Apparently the kinematic model *is* consistent with a dynamical balance in the equilibrium range, but only for one particular value of D, namely $D = 1$. And this result holds for any nonlinear wave–wave interaction with $q > 1$. A more physical understanding of this result is sought next.

4. Discussion

So what does a value of $D = 1$ mean physically? When $D = 1$, the formula (2.29) for the length of breaking fronts with scales in the range l_Λ to $l_\Lambda + \mathrm{d}l_\Lambda$ per unit area becomes

$$F(l_\Lambda)\mathrm{d}l_\Lambda = (A_0/l_\Lambda^2)\mathrm{d}l_\Lambda, \tag{4.1}$$

where $A_0 = F_0 l_0$. Hence the total length of small breaking waves is greater than the total length of large breaking waves. Now consider

$$A(l_\Lambda)\mathrm{d}l_\Lambda = F(l_\Lambda)\mathrm{d}l_\Lambda \times l_\Lambda = (A_0/l_\Lambda)\mathrm{d}l_\Lambda, \tag{4.2}$$

the total length of breaking waves with scales in the range l_Λ to $l_\Lambda + \mathrm{d}l_\Lambda$ per unit area of sea surface multiplied by the width of such waves, which might be thought of as the *fraction of area* covered by breaking waves in a given band of scales. And A_0 is the fraction of sea surface covered by waves with scales greater than l_0. Notice that, although we speak of a 'fraction', if the breaking waves overlap then it is possible that $A(l_\Lambda) > 1$. Now if l_s is the scale of the smallest breaking waves in the equilibrium range and if $A^>(l_s)$ is the fraction of sea surface covered by breaking waves with scales greater than l_s, then when $D = 1$

$$A^>(l_s) = \int_{l_s}^{l_0} A(l_\Lambda)\,\mathrm{d}l_\Lambda = A_0 \ln(l_0/l_s). \tag{4.3}$$

The value $D = 1$ is the limiting case for $A^>$: if $D > 1$ then $A^>$ increases as a power law with l_0/l_s; if $D < 1$ then $A^>$ asymptotes to a constant value, equal to A_0/D, as l_0/l_s increases; finally, if $D = 1$ then $A^>$ increases indefinitely with l_0/l_s, but only logarithmically.

Furthermore, $D = 1$ means that the ratio of the fraction of area covered by breaking waves in the band l_Λ and $l_\Lambda + \mathrm{d}l_\Lambda$ to the fraction of area covered by waves in the rescaled band sl_Λ and $s(l_\Lambda + \mathrm{d}l_\Lambda)$ is independent of s, i.e.

$$\frac{A(l_\Lambda)\mathrm{d}l_\Lambda}{A(sl_\Lambda)\mathrm{d}(sl_\Lambda)} = 1, \tag{4.4}$$

so that $D = 1$ implies that breaking waves from each band of scales covers that same fraction, A_0, of the sea surface.

Hence the equilibrium described here is one where the breaking waves fill the same fraction of area independently of their size. This property we call *space-filling saturation*. This usage of 'space filling' is consistent with the usage in Kolmogorov's model of the inertial range of turbulence where the turbulent eddies fill the same fraction of space independently of their size and are called space filling (see e.g. Frisch 1995). Our usage of 'saturation' follows Phillips (1958) as discussed below.

When $D = 1$ equation (2.30) for the two-dimensional wavenumber spectrum is

$$\Psi(\boldsymbol{k}) = \left\{\tfrac{1}{2}(2\pi)^{3/2}(\alpha_\Lambda \beta_\Lambda)^2\right\} A_0 \Theta(\theta) k^{-4}, \tag{4.5}$$

which decays as k^{-4}. The angular variation is determined by the probability density of the angular distribution of breaking-wave fronts, namely $\Theta(\theta)\mathrm{d}\theta$, the probability that a breaking-wave front propagates between the angles θ and $\theta + \mathrm{d}\theta$ to the wind direction. The coefficient multiplying these factors depends on the self-similar geometry of breaking waves through α_Λ, the average change in slope at a breaking crest, and through β_Λ, the average slope of breaking waves. Finally the spectrum depends on A_0, the fraction of sea surface covered by breaking waves of a given band of scales.

Phillips (1958) developed a model for the equilibrium range based on the idea that waves break when the acceleration at the crest exceeds some fraction of g. Such reasoning, augmented by dimensional arguments, leads to $\Psi(\boldsymbol{k}) = \text{const} \times k^{-4}$. Phillips (1958) also suggested that such a spectrum can be associated with discontinuities in wave slope at the breaking crests. But our detailed calculations show this argument holds only for one-dimensional data; in two-dimensions, which is relevant to the ocean, the basic decay is as k^{-5} for breaking-wave fronts with line segments of discontinuity in slope. Hence our result that $\Psi(\boldsymbol{k})$ decays as k^{-4} is non-trivial and is based on the finding that breaking waves adjust so that at equilibrium a constant fraction of area is covered by breaking waves of a given band of scales. We have termed this space-filling saturation. Phillips (1958) also used the term saturation, but with a different meaning: he meant that individual waves saturate when they break; we use the term space-filling saturation to mean a constant fraction of sea surface covered by breaking waves, so it is the spatial distribution of breaking waves that is saturated.

Banner (1990) surveyed laboratory and field data and found empirically that, in the windward direction, θ_0, the spectra decayed as

$$\Psi(k, \theta_0) = 0.45 \times 10^{-4} (U_0/c_p)^{1/2} k^{-4}, \tag{4.6}$$

where U_0 is the surface wind speed and c_p is the phase speed of waves at the peak in the spectrum. Hence the theoretical model developed here gives the same k^{-4} variation as the data.

The data analysed by Banner (1990) also suggest that the coefficient multiplying the k^{-4} is wind dependent, varying as $(U_0/c_p)^{1/2}$. How can such a wind dependence enter the present model (4.5)? Firstly, it is unlikely that the wind strongly affects the geometry of the breakers in the bulk of the equilibrium range: the wind affects the water motions primarily through the surface pressure gradient, which scales as $O(\rho_a U_0^2/l_\Lambda)$ for breaking waves of scale l_Λ, whereas the inertial gradient in the water, which scales as $O(\rho_w(\beta_\Lambda c_\Lambda)^2/l_\Lambda)$, is much larger than this pressure gradient when $U_0/c_\Lambda \gtrsim 10$ (when $\beta_\Lambda \approx \frac{1}{3}$). Hence, if $U_0 = 10$ m s^{-1}, breaking waves with scales greater than about 10 cm are not significantly affected by the air flow. So that we expect α_Λ and β_Λ to be independent of wind speed. The angular spreading of the spectrum with wavenumber may depend on wind speed (e.g. Donelan, Hamilton & Hui 1986), but the variation of $\Theta(\theta)$ cannot be great. Hence A_0 must account for most of the variation with U_0/c_p. It certainly seems reasonable for A_0, the fraction of sea-surface area covered by breaking waves in a band of scales, to increase with wind speed. And A_0 might be expected to decrease with c_p: as c_p increases so does the extent of the equilibrium range and hence the range of wavenumbers that dissipate energy, so the energy dissipated per unit wavenumber decreases, hence the coverage of breaking waves per unit wavenumber (i.e. A_0) should decrease with c_p.

Providing a theoretical reasoning for how the spectrum depends on U_0/c_p is more difficult. We could argue, following Phillips (1985), that the wind input also scales as

the nonlinear flux divergence and dissipation due to breaking in (3.1). This is certainly possible in the present framework: as discussed above in a scale-invariant equilibrium range all three terms can balance. But to use such reasoning explicitly would require knowledge of energy input into breaking waves. While some attempts have been made to model air flow over breaking waves (e.g. Maat & Makin 1992), the results remain tentative and most models of air flow over waves have been restricted to sinusoidal waves (for recent developments see e.g. Belcher & Hunt 1993; Mastenbroek *et al.* 1996), and so it is not known if the wind input to breaking waves is large enough to be important in the spectral balance. This question is left for future study.

5. Frequency spectrum

The frequency spectrum of the waves, $\Phi(\sigma)$, is determined from the variation of wave elevation with time and is defined by

$$\Phi(\sigma) \equiv \int_{-\infty}^{\infty} \overline{\zeta(t)\zeta(t+\tau)} e^{i\sigma\tau} d\tau = \frac{(2\pi)^2}{\bar{T}} \overline{|\hat{\zeta}(\sigma)|^2}, \tag{5.1}$$

where $\hat{\zeta}(\sigma)$ is the Fourier transform of $\zeta(t)$ and the overbar denotes averaging over realizations and over time $\bar{T}$, the length of the record. Previous studies (e.g. Kitaigorodskii 1983; Phillips 1985) have considered the waves to be freely propagating Fourier components, with only weak nonlinear interactions, and so they could obtain $\Phi(\sigma)$ from $\Psi(\boldsymbol{k})$ by using the linear dispersion relation to convert $\boldsymbol{k}$ into σ. Here we have highlighted the key role played by sharp-crested breaking waves, whose shapes have a range of Fourier components that all propagate at the same speed. So here it is not correct to convert wavenumbers into frequencies using a dispersion relation because $\Psi(\boldsymbol{k})$ has contributions from sharp-crested waves of different scales, which have different phase speeds. Indeed it is not clear that a phase velocity can even be defined in Fourier space!

Instead we calculate the frequency spectrum in the equilibrium range by using kinematic arguments for one-dimensional signals developed in §2.2. Then $F(l)dl$, the length of breaking waves of scales in the range l to $l + dl$ per unit area, is related to $M(\tau_\Lambda)d\tau_\Lambda$, the expected number of breaking waves passing the measuring point per unit time. Finally the result of the previous section that $D = 1$ is used to determine the form of $\Phi(\sigma)$ in the equilibrium range.

5.1. *Kinematics*

As before the wave surface, $\zeta(t)$, is written as a sum of smooth waves together with sharp-crested waves

$$\zeta(t) = \zeta_s(t) + \sum_{mn} a_{nm} \Lambda_{nm}((t - t_{0mn})/\tau_n), \tag{5.2}$$

where a_{nm} is the amplitude of the nmth wave, τ_n is a timescale of the wave and t_{0nm} is the time at which the peak in the mnth wave passes the measuring point. The analysis of §2.1 then shows that the Fourier transform of the surface is dominated by the singularities at the crests, so that

$$\hat{\zeta}(\sigma) = \frac{1}{2\pi\sigma^2} \sum_{mn} \alpha_{mn}\beta_{mn} c_n e^{i\phi_{mn}} H(\sigma\tau_n - 1) + o(\sigma^{-2}). \tag{5.3}$$

Notice that for temporal data, although the α_Λ is the same as in (2.6), the factor of l_n becomes τ_n. But then $\tau_n^{-1} = c_n l_n^{-1}$, where c_n is the phase speed, so that

$a_{mn}/\tau_n = c_n a_{mn}/l_n = \beta_{mn} c_n$. This new factor of c_n arises from a Doppler shift of the wave, which changes the apparent jump in slope at the wave crest: faster waves appear to have a greater jump in slope as they pass the measuring point more quickly. This Doppler shift proves to be important in determining the frequency spectrum.

Going immediately to a collection of Λ-crests with a continuous distribution of timescales, so that $M(\tau_\Lambda)\mathrm{d}\tau_\Lambda$ is the expected number of Λ-crests with timescales in the range τ_Λ to $\tau_\Lambda + \mathrm{d}\tau_\Lambda$ passing the measuring point per unit time, the frequency spectrum becomes

$$\Phi(\sigma) = \frac{\alpha_\Lambda{}^2 \beta_\Lambda{}^2}{\sigma^4} \int_0^{\tau_0} M(\tau_\Lambda) c_\Lambda^2(\tau_\Lambda) H(\sigma\tau_\Lambda - 1)\mathrm{d}\tau_\Lambda. \tag{5.4}$$

Here τ_0 is the outer timescale. Recall that for the one-dimensional spectra the basic decay is like σ^{-4}. Any modification to this law can be found once $M(\tau_\Lambda)\mathrm{d}\tau_\Lambda$ is computed.

5.2. *Calculation of* $M(\tau_\Lambda)\mathrm{d}\tau_\Lambda$

The next step is to relate the expected length of breaking waves of a given band of lengthscales per unit area to the expected number of waves of a given band of timescales passing the measurement point per unit time, i.e. relating $F(l_\Lambda)\mathrm{d}l_\Lambda$ to $M(\tau_\Lambda)\mathrm{d}\tau_\Lambda$.

Breaking waves on the ocean are transient features and so to relate $F(l_\Lambda)$ to $M(\tau_\Lambda)$ requires information on temporal properties of the breakers. First, field experiments by Ding & Farmer (1994) and laboratory experiments cited in Melville (1994) suggest that the lifetime of a breaker, T_Λ, scales on the period of the wave (i.e. the time it takes the breaker to travel its lengthscale l), i.e. $T_\Lambda \sim \tau_\Lambda$. Secondly, Duncan's (1981) experiments show that the phase speed of the breaking waves is given by $c_\Lambda = (\mathrm{g}l_\Lambda)^{1/2}$. Both of these findings are consistent with individual breaking waves being self-similar.

Now consider a snapshot of the wave field at some instant of time. Focus on the breaking waves in this snapshot that have lengthscales in the range l_Λ to $l_\Lambda + \mathrm{d}l_\Lambda$. Consider a strip of sea surface centred on the observation point, X, and at angle φ to the wind, and of width f_Λ and length d, the distance travelled by a Λ-crest in its lifetime. Then any Λ-crest travelling at angle φ to the wind and whose centre is within the strip and will be detected at X. Now, the expected number of Λ-crests with scales between l_Λ and $l_\Lambda + \mathrm{d}l_\Lambda$ in this strip is $M(l_\Lambda)\mathrm{d}l_\Lambda \times f_\Lambda d$. Then in a time $T = d/c_\Lambda$ these Λ-crests traverse the strip, and hence all Λ-crests within the strip are detected at X. Strips are then averaged over angle φ weighted by $\Theta(\varphi)$ which integrates to 1. The expected number of Λ-crests with sizes from l_Λ to $l_\Lambda + \mathrm{d}l_\Lambda$ detected at X per unit time is then

$$M_T(l_\Lambda)\mathrm{d}l_\Lambda \sim M(l_\Lambda)\mathrm{d}l_\Lambda \times f_\Lambda d \times 1/T \sim c_\Lambda(l_\Lambda)F(l_\Lambda)\mathrm{d}l_\Lambda. \tag{5.5}$$

The final step is to use the definition $M_T(l_\Lambda)\mathrm{d}l_\Lambda = M(\tau_\Lambda)\mathrm{d}\tau_\Lambda$. Hence $M(\tau_\Lambda)\mathrm{d}\tau_\Lambda$ can be calculated in terms of τ_Λ using the dispersion relation $\tau_\Lambda^{-1} = c_\Lambda l_\Lambda^{-1} = (\mathrm{g}/l_\Lambda)^{1/2}$, which shows that

$$M(\tau_\Lambda)\mathrm{d}\tau_\Lambda = v\frac{2A_0}{\tau_0^2}\left(\frac{\tau_0}{\tau_\Lambda}\right)^{2D}\mathrm{d}\tau_\Lambda, \tag{5.6}$$

where v is a coefficient that accumulates from the scalings given above.

5.3. *Frequency spectrum*

The frequency spectrum of the waves can now be calculated. The integrand in (5.4) becomes

$$c_\Lambda^2 M(\tau_\Lambda)\mathrm{d}\tau_\Lambda = 2\mathrm{g}^2 A_0 v \left(\tau_0/\tau_\Lambda\right)^{2(D-1)} \mathrm{d}\tau_\Lambda, \tag{5.7}$$

since $c_\Lambda = \mathrm{g}\tau_\Lambda$. Integration of (5.4) shows that, when $D \neq \frac{3}{2}$,

$$\Phi(\sigma) = \frac{{\alpha_\Lambda}^2 {\beta_\Lambda}^2}{\sigma^4} 2\mathrm{g} c_0 A_0 v \frac{1}{3-2D} \left\{ 1 - \left(\frac{1}{\tau_0 \sigma} \right)^{3-2D} \right\}. \tag{5.8}$$

Hence when $D < \frac{3}{2}$, and in particular when $D = 1$, the first term dominates over the second when $\sigma\tau_0 \gg 1$, because $1/(\sigma\tau_0)^{3-2D} \to 0$, and the frequency spectrum becomes

$$\Phi(\sigma) = 2{\alpha_\Lambda}^2 {\beta_\Lambda}^2 \nu A_0 c_0 \mathrm{g}\sigma^{-4}. \tag{5.9}$$

The frequency spectrum is dominated by the Λ-crests with the large timescales, greater than τ_0, which also have the largest lengthscales, greater than l_0, because the energy in the smaller Λ-crests is too small to make a contribution to the frequency spectrum (cf. the discussion of figure 2*b*). This dominance of the frequency spectrum by the largest Λ-crests occurs through a combination of two effects. First, the number of Λ-crests in a given band of timescales passing the measuring point per unit time increases as the timescale decreases when $D = 1$. But, secondly, the square of the speed of the waves multiplies this factor. This second factor arises because the slope of the waves observed in a time series is Doppler shifted, so that faster waves appear to have steeper slopes, and in particular have a greater jump in slope at their crest. This Doppler effect means that $c_\Lambda^2 M(\tau_\Lambda)$ is independent of timescale, τ_Λ, and hence the integrated effect is that the small scales do not contribute to the frequency spectrum. This leads to the suprising conclusion that, in the equilibrium range, the frequency spectrum contains information about only a small fraction of the total wave field, namely the largest breaking waves.

According to the present model the frequency spectrum varies in the equilibrium range as σ^{-4}. Data presented in Phillips (1985) show convincingly that measured spectra vary in the equilibrium range as

$$\Phi(\sigma) = \text{constant} \times u_* \mathrm{g}\sigma^{-4}. \tag{5.10}$$

Hence a second objective of this paper has been achieved and the present model gives a frequency spectrum that varies correctly with σ.

6. Conclusions

We have developed a theory for the equilibrium range of wind waves by arguing that wave breaking is the controlling process in the equilibrium range and that breaking waves have a near discontinuity in slope at their sharp crests. At high wavenumbers the wavenumber spectrum of the waves, $\Psi(\boldsymbol{k})$ is then dominated by this singularity at the breaking crests. Hence our conception of the wave field is that, at low wavenumbers, wave breaking is rare, but becomes more common as the wavenumber increases. Hence the lower wavenumber limit of the equilibrium range is the wavenumber where the energy in breaking waves equals the energy in the non-breaking waves. At higher wavenumbers still, in the equilibrium range, the energy, and hence also the spectrum, is dominated by the breaking waves.

The theory is based on the assumption that the equilibrium range is scale invariant,

in the sense defined in §1.2. This assumption implies that individual breaking waves have self-similar shapes and also determines that the distribution of breaking waves, parameterized by the total length of breaking-wave fronts in a given band of scales per unit area of sea surface, $F(l_\Lambda)\mathrm{d}l_\Lambda$, varies with l_Λ as a power law, characterized here with exponent D.

A kinematic calculation of such a scale-invariant distribution of self-similar two-dimensional sharp-crested breaking waves shows that the two-dimensional wavenumber spectrum is

$$\Psi(\boldsymbol{k}) = \tfrac{1}{2}(2\pi)^{3/2}(\alpha_\Lambda\beta_\Lambda)^2\frac{1}{D}\Theta(\theta)A_0 l_0^{D-1}\frac{1}{k^{5-D}}, \tag{6.1}$$

which varies as k^{-5+D}.

The exponent D is determined by invoking an equilibrium balance in the dynamical processes that control the waves. This dynamical balance is also assumed to be scale invariant. Physically, the balance implies that the amplitudes of non-breaking waves in the equilibrium range are increased by nonlinear wave–wave interactions and possibly also by wind input of energy. This leads to local excesses of wave energy, and thence to sharp-crested breaking waves that dissipate wave energy. Hence for an equilibrium balance the dissipation rate is proportional to the flux divergence due to wave–wave interactions. This balance, together with an estimate of energy dissipation based on experiments by Duncan (1981), determines that

$$D = 1. \tag{6.2}$$

The result $D = 1$ means that the fraction of sea surface covered with waves of a band of scales near l_Λ, defined here as the total length of breaking wave fronts in the band multiplied by the cross-sectional scale l_Λ, is a coefficient, A_0, that is independent of l_Λ. Hence the equilibrium is a space-filling saturation in the following sense. Waves of a given scale grow with fetch or duration. Subsequently they begin to break, and the number of breaking waves increases with the fetch or duration until enough waves of that scale are breaking to balance the flux from wave–wave interactions, and possibly further wind input. Then saturated equilibrium is attained. The value of A_0 may depend on wind speed, but further work on air flow over breaking waves is needed to clarify how. The value of $D = 1$ determines that $\Psi(\boldsymbol{k})$ varies as k^{-4}, in agreement with data presented by Banner (1990).

The frequency spectrum, $\Phi(\sigma)$, is obtained by calculating the average number of breaking waves passing a measuring point per unit time. The breaking waves are affected by a Doppler shift so that larger breakers, which travel at larger phase speeds, appear to have a change in slope at their crests that is larger than the small breakers. The result is that $\Phi(\sigma)$ is controlled by only the largest breaking waves, the smaller breaking waves being too infrequent and carrying too little energy to register in the spectrum. Clearly the frequency spectrum contains little or no information about the small-scale wave field. Our calculations show that

$$\Phi(\sigma) = 2{\alpha_\Lambda}^2{\beta_\Lambda}^2 \nu A_0 c_0 \mathrm{g}\sigma^{-4}, \tag{6.3}$$

which has the same σ^{-4} variation as the data presented in Phillips (1985).

Hence the present model explains why $\Psi(\boldsymbol{k}) \sim k^{-4}$ and $\Phi(\sigma) \sim \sigma^{-4}$, which previous models found difficult to explain because they were based on sinusoidal waves that satisfied the linear dispersion relationship.

The suprising finding that only large breaking waves contribute to $\Phi(\sigma)$ suggests a possible way of distinguishing the present theory from previous work of Phillips

(1985), which assumed that waves in the equilibrium range are free sinusoidal modes. Time series of the water-surface elevation could be analysed, for example using wavelet tranforms, to identify the sharp-crested breaking waves. If the small-scale waves were removed from the sequence, then the present theory shows that the frequency spectrum would be unchanged. In contrast the previous theories would suggest that the high-frequency part of the spectrum would be reduced to zero.

The present theory also suggests that it might be more difficult to observe in data the k^{-4} variation in $\Psi(\boldsymbol{k})$ than the σ^{-4} variation in $\Phi(\sigma)$. To observe a k^{-4} variation requires that the spatial pattern of the wave surface has been sampled sufficiently well that the statistical properties of the breaking waves are well resolved through the whole range of scales of the equilibrium range because the k^{-4} variation is dependent on contributions to the spectrum from breaking waves over a wide range of scales. Indeed under-sampling or poor resolution of the small scales might make the spectrum vary more like k^{-5}, or some power between 4 and 5. In contrast the σ^{-4} variation is produced as soon as the large scale breaking waves are detected. This may explain why the data presented in Phillips (1985) for the frequency spectrum certainly show a convincing σ^{-4} variation, whereas the data in Banner (1990) shows a k^{-4} variation over only a short range of wavenumbers.

It is a pleasure to acknowledge the generous hospitality shown to S.E.B. by Owen Phillips during a visit to Johns Hopkins University during the summer of 1995 when this work was begun and to thank him for the fruitful conversations. S.E.B. was supported during this visit by CEC under contract EV5V–CT93–0291. J.C.V. is grateful to the Royal Society for financial support.

REFERENCES

Banner, M. L. 1990 Equilibrium spectra of wind waves. *J. Phys. Oceanogr.* **20**, 966–984.

Banner, M. L. & Peregrine, D. H. 1993 Wave breaking in deep water. *Ann. Rev. Fluid Mech.* **25**, 373–397.

Belcher, S. E. & Hunt, J. C. R. 1993 Turbulent shear flow over slowly moving waves. *J. Fluid Mech.* **251**, 109–148.

Bonmarin, P. 1989 Geometrical properties of deep-water breaking waves. *J. Fluid Mech.* **209**, 405–433.

Ding, L. & Farmer, D. M. 1994 Observations of breaking surface wave statistics. *J. Phys. Oceanogr.* **24**, 1368–1387.

Donelan, M. A., Hamilton, J. & Hui, W. H. 1985 Directional spectra of wind-generated waves. *Phil. Trans. R. Soc. Lond.* A **315**, 509–562.

Duncan, J. H. 1981 An experimental investigation of breaking waves produced by a towed hydrofoil. *Proc. R. Soc. Lond.* A **377**, 331–348.

Frisch, U. 1995 *Turbulence.* Cambridge University Press.

Gilbert, A. 1988 Spiral structures and spectra in two-dimensional turbulence. *J. Fluid Mech.* **193**, 475–497.

Glazman, R. E. & Weichman, P. B. 1989 Statistical geometry of a small surface patch in a developed sea. *J. Geophys. Res.* **94**, C4, 4998–5010.

Kitaigorodskii, S. A. 1983 On the theory of the equilibrium range in the spectrum of wind-generated gravity waves. *J. Phys. Oceanogr.* **13**, 816–827.

Komen, G. J., Hasselmann, S. & Hasslemann, K. 1984 On the existence of a fully developed windsea spectrum. *J. Phys. Oceanogr.* **14**, 1271–1285.

Lighthill, M. J. 1958 *An Introduction to Fourier Analysis and Generalised Functions.* Cambridge University Press.

Maat, N. & Makin, V. K. 1992 Numerical simulation of air-flow over breaking waves. *Boundary-Layer Met.* **60**, 77–93.

MAKIN, V. K., KUDRYATSEV, V. N. & MASTENBROEK, C. 1995 Drag of the sea surface. *Boundary-Layer Met*. **73** 159–182.

MASTENBROEK, C., MAKIN, V. K., GARAT, M. H. & GIOVANANGELI, J. P. 1996 Experimental evidence of the rapid distortion of turbulence in air flow over water waves. *J. Fluid Mech*. **318**, 273–302.

MELVILLE, W. K. 1994 Energy dissipation by breaking waves. *J. Phys. Oceanogr*. **24**, 2041–2049.

MELVILLE, W. K. 1996 The role of surface-wave breaking in air–sea interaction. *Ann. Rev. Fluid Mech*. **28**, 279–321.

OREY, S. 1970 Gaussian sample functions and the Hausdorff dimension of level crossings. *Z. Wahrscheinlichkeitstheorie verw. Geb*. **15**, 249.

PHILLIPS, O. M. 1958 The equilibrium range in the spectrum of wind-generated waves. *J. Fluid Mech*., **4**, 426–434.

PHILLIPS, O. M. 1977 *Dynamics of the Upper Ocean*. Cambridge University Press.

PHILLIPS, O. M. 1985 Spectral and statistical properties of the equilibrium range in wind-generated gravity waves. *J. Fluid Mech*. **156**, 505–531.

PIERSON, W. J. 1955 Wind generated gravity waves. *Adv. Geophys*. **2**, 93–178.

RAPP, R. J. & MELVILLE, W. K. 1990 Laboratory measurements of deep-water breaking waves. *Phil. Trans. R. Soc. Lond*. A **331**, 735–800.

SHEN, Z., WANG, W. & MEI, L. 1994 Finestructure of wind waves analysed with wavelet transforms. *J. Phys. Oceanogr*. **24**, 1085–1094.

TOBA, Y. 1973 Local balance in the air–sea boundary layer. III. On the spectrum of wind waves. *J. Oceanogr. Soc. Japan* **29**, 209–220.

VASSILICOS, J. C. 1995 Anomolous diffusion of isolated flow singularities and of fractal or spiral structures. *Phys. Rev*. E **52**, R5753–5756.

VASSILICOS, J. C. & HUNT, J. C. R. 1991 Fractal dimensions and spectra of interfaces with application to turbulence. *Proc. R. Soc. Lond*. A **435**, 505–534.